Published in final edited form as:
J Immunol. 2011 September 15; 187(6): . doi:10.4049/jimmunol.1101447.

Caveolin-1 Orchestrates TCR Synaptic Polarity, Signal Specificity, and Function in CD8 T Cells

Tamar Tomassian[*,†], **Lisa A. Humphries**[*], **Scot D. Liu**[*], **Oscar Silva**[*], **David G. Brooks**[*,†], and **M. Carrie Miceli**[*,†]

[*]Department of Microbiology, Immunology, and Molecular Genetics, David Geffen School of Medicine and College of Letters and Sciences, University of California, Los Angeles, Los Angeles, CA 90095

[†]Molecular Biology Institute, University of California, Los Angeles, Los Angeles, CA 90095

Abstract

TCR engagement triggers the polarized recruitment of membrane, actin, and transducer assemblies within the T cell–APC contact that amplify and specify signaling cascades and Teffector activity. We report that caveolin-1, a scaffold that regulates polarity and signaling in nonlymphoid cells, is required for optimal TCR-induced actin polymerization, synaptic membrane raft polarity, and function in CD8, but not CD4, T cells. In $CD8^+$ T cells, caveolin-1 ablation selectively impaired TCR-induced NFAT-dependent NFATc1 and cytokine gene expression, whereas caveolin-1 re-expression promoted NFATc1 gene expression. Alternatively, caveolin-1 ablation did not affect TCR-induced NF-κB–dependent Iκbα expression. Cav-$1^{-/-}$ mice did not efficiently promote CD8 immunity to lymphocytic choriomeningitis virus, nor did cav-$1^{-/-}$ OT-1^+ $CD8^+$ T cells efficiently respond to *Listeria mono-cytogenes*-OVA after transfer into wild-type hosts. Therefore, caveolin-1 is a T cell-intrinsic orchestrator of TCR-mediated membrane polarity and signal specificity selectively employed by CD8 T cells to customize TCR responsiveness.

T cells have the remarkable capacity to sense subtleties in Ag quality and presentation and to respond appropriately in one of several manners. Specific TCR binding to peptide-bound MHC on APC can stimulate a T cell to become tolerant or activated, differentiate into one of several effector T cell lineages, or selectively synthesize and secrete T cell cytokines or cytotoxic effectors (1–3).

The TCR couples to downstream signal transduction pathways and functional output through the induced association and activation of nonreceptor tyrosine kinases Lck and ZAP70. These proximal kinases, in turn, activate effector-signaling cascades responsible for actin remodeling, polarized membrane and effector protein trafficking, gene expression, and T cell functional responses (1–3). Although it is well established that the TCR can couple to a number of downstream transducer pathways with discrete capacities to impact T cell activities, mechanisms by which TCR engagement is selectively channeled toward the

Address correspondence and reprint requests to Dr. M. Carrie Miceli, Department of Microbiology, Immunology, and Molecular Genetics, 277B Biological Science Research Building, University of California, Los Angeles, School of Medicine, 615 Charles E. Young Drive East, Los Angeles, CA 90095-1570. cmiceli@ucla.edu.

The online version of this article contains supplemental material.

Disclosures
The authors have no financial conflicts of interest.

activation of a subset of downstream transducer cascades are only now beginning to be elucidated.

TCR Ag recognition induces the formation of a polarized immunological synapse at the T cell–APC junction, providing context for TCR signal transduction and a target for polarized membrane traffic and T effector molecule delivery (3). The recruitment and organization of membrane microdomains, scaffold proteins, and actin-dependent macromolecular assemblies within the synaptic contact help set tunable thresholds, guide TCR signal specificity, and dictate fate and functional output (1–4). During activation, TCRs engaged at the periphery of the contact form actin-dependent microclusters that traffic toward a central supra-molecular activation cluster (3).

The assembly and composition of T cell synapses differ throughout T cell development and differentiation and between mature T effector subsets (1, 3). In some T cell subsets, cholesterol and sphingolipid-rich raft membrane microdomains translocate to the synapse, where they cluster and concentrate TCR signal transducers, exclude negative regulators, and modify actin-mediated synaptic organization (2, 5, 6). However, mechanisms by which different T cell subsets specialize synapses to set signaling thresholds and specify TCR output are not well understood.

Caveolin-1 is a key organizer of membrane specializations that orchestrate signal transduction and membrane and protein traffic in polarized epithelial cells, neuronal synapses, and other cell types (7– 22). By directly interacting with cholesterol and membrane raft-associated sphingolipids (23, 24), caveolin-1 promotes the assembly and stability of plasma membrane raft microdomains in which specific transducers preferentially partition and that serve as platforms for signal transduction (21, 23–25). Additionally, caveolin-1 orchestrates the assembly and activity of multimolecular signaling complexes through its activity as a protein scaffold, binding a wide array of signal transducers through interactions with phosphorylated tyrosine 14 or the scaffolding domain (aa 82–101) within caveolin-1 (23, 26). Many of the proteins identified as caveolin-1 binding partners in non-T cells have been implicated in TCR-regulated membrane dynamics, actin reorganization, signaling, and function (14, 17, 18, 20, 27). However, initial reports that T lineage cells may not express caveolin-1 discouraged investigation of a potential role for caveolin-1 as an organizer of TCR synaptic membrane dynamics and signal transduction (28–32).

Based on studies defining caveolin-1 as an orchestrator of cell polarity, membrane traffic, and signal transduction in other cell types, we hypothesized that caveolin-1 might regulate similar processes in T cells. In this study, we provide data demonstrating caveolin-1 expression in primary T lineage cells. We define a role for caveolin-1 in orchestrating specific T cell responses to Ag receptor engagement in CD8, but not CD4, T cells despite expression in both T cell subsets. Caveolin-1 expression facilitated the polarized redistribution of membrane rafts to the APC–T cell contact and the Ag-induced actin polymerization required for this redistribution. Caveolin-1 expression selectively enhanced TCR-induced CD8 T cell NFAT but not NF-κB–dependent gene expression. Accordingly, cav-$1^{-/-}$ CD8 T cells demonstrated defective TCR-triggered proliferation, expansion, CTL activity, IFN-γ and TNF-α production, and a diminished ability to clear a lymphocytic choriomeningitis virus (LCMV) challenge in vivo. T cells lacking caveolin-1 remained competent to affect these functions when triggered by PMA and ionomycin, highlighting a role for caveolin-1 in coupling TCR engagement to select downstream signal transduction and effector pathways. These findings elucidate caveolin-1 as an orchestrator of TCR signal specificity, actin reorganization, and synaptic polarity in CD8, but not CD4, T cells.

Materials and Methods

Mice

Cav-1$^{-/-}$ mice on a mixed C57BL/6*129/sv*SJL background (Cav1tm1Mls/J; The Jackson Laboratory) were backcrossed 14 generations with C57BL/6 mice to produce cav-1$^{-/-}$C57BL/6 mice. cav-1$^{-/-}$ OT-1 mice were generated by crossing cav-1$^{-/-}$C57BL/6 mice with OT-1 TCR-transgenic mice. Mice were genotyped using protocols available through The Jackson Laboratory (Cav1tm1Mls; standard PCR). Experiments followed an approved protocol of the University of California, Los Angeles, Chancellor's Animal Research Committee.

Immunoblotting analysis

Cells were lysed on ice for 30 min in TNE buffer (50 mM Tris, 1% Nonidet P-40, 2 mM EDTA) containing protease and phosphatase inhibitors. Samples were separated on 12% SDS-PAGE, transferred to nitrocellulose, and immunoblotted with a rabbit polyclonal Ab directed against the first 97 (1–97) aa of caveolin-1 (610059; BD Pharmingen) (Fig. 1*A*, 1*B*), a rabbit polyclonal Ab directed against 20 aa in the N terminus of caveolin-1 (sc-894; Santa Cruz Biotechnology) (Fig. 1*C*), or a mouse mAb directed against full-length caveolin-1 (610406; BD Pharmingen) (Fig. 4*C*). Abs directed against Erk2 (C-14) (sc-154, rabbit polyclonal Ab; Santa Cruz Biotechnology) and p38a (C-20) (sc-535, rabbit polyclonal Ab; Santa Cruz Biotechnology) were used to normalize for protein loading.

FACS analysis

Thymocytes and splenocytes from mice (6.2 and/or 8 wk) were counted and stained with directly fluorescently labeled anti-CD3, -CD4, and -CD8 Abs (BD Pharmingen) using standard protocols, acquired on an FACSCalibur (BD Biosciences), and analyzed using CellQuest software (BD Bio-sciences). For cytokine expression, 1 μl GolgiPlug (BD Pharmingen) was added to wells 5 h before harvest; cells were subsequently stained with anti-CD8 Ab, fixed, permeabilized with Cytofix/Cytoperm (BD Pharmingen), and stained with anti–IFN-γ Ab (BD Pharmingen).

CTL assay

Purified wild-type or cav-1$^{-/-}$CD8^{+} cells were primed with 2 μg anti-CD3 and 5 μg anti-CD28 Abs for 72 h, counted, and incubated with P815 cells at indicated E:T ratios for 4 h. Cell-mediated cytotoxicity was determined using the Cytoscan-LDH Cytotoxicity Assay Kit (Genotech) and percent cytotoxicity calculated according to the manufacturer's instructions.

Proliferation assays

Splenocytes from C57BL/6 mice were enriched for CD8 cells using a CD8 isolation kit (Miltenyi Biotec) and magnetic cell sorting (AutoMACS). Purity ranged from 85–95% CD8 T cells. For [^{3}H]thymidine assay, 2×10^{5} CD8 cells were cultured with 2×10^{5} Ab-coated beads (50 μg/ml anti- CD3 with 200 μg/ml anti-CD28) for 72 h. A total of 1 μCi [^{3}H]thymidine (Amersham Biosciences) per well was added 8 h before harvesting cells onto glass fiber filters (PerkinElmer) with an automated cell harvester (Tomtec). Incorporated radioactivity was measured using a β-plate scintillation counter.

Alternatively, CD8 cells were labeled with CFSE (Invitrogen) and stimulated with plate-bound anti-CD3 (2 μg/ml) and anti-CD28 (2–5 μg/ ml) Abs for indicated times, after which cells were collected and stained with anti-CD8 Ab (BD Pharmingen). Average stage of division was calculated by analyzing CFSE histograms gated on live CD8 cells using the

following equation: average stage = ([(% undivided) + (2 × % division 1) + (3 × % division 2) + xxx)]/100) − 1.

Fluorescent microscopy

Purified wild-type or cav-$1^{-/-}$ OT-$1^{+}CD8^{+}$ cells were incubated with APCs for 30 min as previously described (33). Cells were stained with 8 μg/ml FITC-conjugated cholera toxin β subunit (Sigma-Aldrich). Images were collected using a Zeiss Axio Imager Z1 microscope (Carl Zeiss). For GM1 clustering, light microscopy was used to identify T cell–APC conjugates. The degree of GM1 synaptic clustering was assessed by a blinded observer. At least 50 conjugates were scored for each condition. Cells were scored positive for synaptic clustering when >60% of the cellular GM1 was relocalized within the half of the T cell proximal to the T cell–APC junction. Two independent experiments were performed, and the mean and SD was calculated to quantitate the percentage of GM1-polarized cells.

Actin polymerization

Purified wild-type or cav-$1^{-/-}$ OT-$1^{+}CD8^{+}$ cells were stimulated with APCs for varying time points and stained for 1 h with 1 μg/ml FITC-conjugated phalloidin (P-5282; Sigma-Aldrich) and anti-CD8β (BD Pharmingen), washed, and analyzed as previously described (33). Change in mean fluorescent intensity of F-actin was calculated by subtracting the mean fluorescent intensity of unstimulated samples from the mean fluorescent intensity of stimulated samples. Peak fold increase in F-actin to cav-$1^{-/-}$ was calculated from peak F-actin levels observed in cav-$1^{+/+}$ and cav-$1^{-/-}$ samples from three independent experiments. Data were analyzed using a two-tailed Student *t* test.

RNA isolation, reverse transcription, and quantitative PCR

Purified wild-type or cav-$1^{-/-}$ OT-$1^{+}CD8^{+}$ cells were stimulated for various times with CD3/CD28 or PMA/ionomycin. Cells were harvested and resuspended in TRIzol (Invitrogen). RNA was reverse-transcribed using Superscript II (Invitrogen), and quantitative PCR (for primer sequences, see Supplemental Table I) was performed and analyzed as previously described (33).

Cloning and retrovirus production

Full-length caveolin-1 was amplified by PCR and cloned into the pMIG retroviral vector (a gift from Sankar Ghosh, Columbia University, New York, NY) using Xho1 and EcoRI restriction sites. Primer sequences are as follows: cav-1α XhoI_For: 5′-ATCGCAATTCTCGAGATGTCTGGGG-GCAAA TACGTAGACTCC-3′; and EcoR1_Rev: 5′-GATATTCAGCAA-CATCCGCATCAGACGCAGAAAGAGATATGAGAATTCACATGT-3′. To generate retrovirus, 293T cells were transfected with pCL-Eco and pMIG-cav1 using TransIT 293 (Mirus) according to the manufacturer's directions. After 48 and 72 h, viral supernatant was harvested and used to spin-infect T cells as described below.

Overexpression of caveolin-1

Purified wild-type or cav-$1^{-/-}$ CD8 cells were expanded on APCs for 3 d. Cells were then transduced with caveolin-1–expressing viral supernatant by spinning cells for 90 min in the presence of 8 μg/ml polybrene (Millipore). Viral supernatant was removed, and media was replaced with complete RPMI 1640 supplemented with 200 U/ml human IL-2 overnight. Cells were spin-infected two additional times. Twenty-four hours after the last spin infection, cells were restimulated for 6 h with 2 μg/ml plate-bound anti-CD3 and 5 μg/ml anti-CD28. Cells were harvested and used for RNA or total cell lysates.

LCMV infections

Mice were inoculated with 2×10^5 PFU Armstrong strain of LCMV. Seven days postinfection, splenocytes were counted and stained with anti-CD8 and $GP_{33–41}$ (KAVYNFATC) or $NP_{396–404}$ (FQPQNGQFI) tetramer (Immunomics) as per the manufacturer's recommendations. Viral titers were quantified as described (34). CTL activity was determined using a standard chromium-release assay of LCMV-infected MC57 target cells (35).

Adoptive transfers

Purified naive wild-type or cav-$1^{-/-}$ OT-1 CD8 cells (2.5×10^5) were transferred into C57BL/6 recipients, and 1 d later, recipient mice were immunized with 5×10^6 CFU *actA*-deficient *Listeria monocytogenes*-OVA (LM-OVA; gift of John Harty, University of Iowa, Iowa City, IA). At day 6 postinfection, splenocytes were obtained, counted, stained with anti-CD8 Ab (BD Pharmingen) and $OVA_{257–264}$ tetramer (Immunomics), and analyzed by FACS.

Ex vivo cytokine expression

For adoptive transfer experiments, 1×10^6 cells from recipient spleens were incubated with PMA/ionomycin or $OVA_{257–264}$ peptide. For LCMV experiments, 1×10^6 splenocytes were stimulated ex vivo with PMA/ionomycin or 2 μg/ml $GP_{33–41}$ or $NP_{396–404}$ peptide. Cells were cultured in the presence of 1 μl GolgiPlug/well for 5 h and subsequently surface stained with anti-CD8 Ab. Cells were fixed and permeabilized using Cytofix/Cytoperm and stained with anti–IFN-γ and –IL-2 Ab. The absolute number of cytokine-producing CD8 T cells was determined by multiplying the frequency of cytokine-positive cells by the total number of cells in the spleen.

Results

Caveolin-1 is expressed in T lineage cells

To determine whether caveolin-1 was expressed in primary T cell populations, T lineage cells were purified from thymus and spleen of wild-type and caveolin-1–deficient (cav-$1^{-/-}$) mice. Immunoblotting total cell lysates with two independent Abs specific for caveolin-1 revealed bands corresponding to the predicted sizes in wild-type, but not cav-$1^{-/-}$ thymus, spleen, and lymph node (Fig. 1*A*–*C*). A rabbit polyclonal Ab directed against the first 97 (1–97) aa of caveolin-1–detected bands migrating at molecular masses corresponding to both α (24 kDa) and β (21 kDa) caveolin-1 isoforms (Fig. 1*A*, 1*B*), whereas a rabbit polyclonal Ab to the α isoform-specific N-terminal 20 aa only recognized a single band migrating at 24 kDa (Fig. 1*C*). Caveolin-1 protein and mRNA encoding caveolin-1 α and β isoforms was detected in both CD4 and CD8 T cell subsets (Fig. 1*C*, 1*D*). We similarly observed caveolin-1 expression in both CD4 and CD8 T cell populations and total splenocytes from wild-type mice, but not in splenocytes from caveolin-1 knockout mice using a second Ab (610059, rabbit polyclonal Ab directed against the first 97 [1–97] aa of caveolin-1; BD Pharmingen), further confirming our findings (not shown). Levels of caveolin-1 expression in T cell subsets were consistently lower than levels observed in control muscle cell lysates (Fig. 1*B*). Thus, previous reports that T lineage cells lack caveolin-1 expression may reflect lower levels of caveolin-1 in T cells, assay sensitivity limits, or expression alterations associated with cell transformation (28, 29). Our findings clearly demonstrate that caveolin-1 is expressed in some primary T lineage cells.

Caveolin-1 is not required for development of thymocytes or peripheral CD4 or CD8 T cells subsets

To determine whether caveolin-1 gene expression influenced developing or mature T cell subpopulations, thymocytes and splenic T cells were isolated from wild-type and cav-$1^{-/-}$ mice and stained with Abs to CD3, CD4, CD8, CD69, CD62L, CD25, and CD5. No differences were observed among the percentage, total cell number, or relative ratios of $CD4^{-}CD8^{-}$ double-negative, $CD4^{+}CD8^{+}$ double-positive, or $CD4^{+}$ and $CD8^{+}$ single-positive subpopulations from wild-type and cav-$1^{-/-}$ thymocytes or splenocytes (Fig. 1*E–J*). Surface levels of CD3, CD4, CD8, CD69, CD62L, CD25, and CD5 proved unaffected between wild-type and cav-$1^{-/-}$ thymocytes or splenic T cells (data not shown). Therefore, development of conventional CD4 and CD8 peripheral T cell subpopulations does not appear to be overtly impaired by loss of caveolin-1 expression, though assessment of caveolin-1 requirements for the development of rare and/or specialized T cell subsets will require additional analysis.

Cav-$1^{-/-}$ CD8, but not CD4, T cells showed defects in TCR-induced proliferation and IFN-γ production

To investigate the effect of caveolin-1 expression on T cell proliferation, mature CD8 and CD4 cells from wild-type or cav-$1^{-/-}$ mice were purified and assessed for their ability to proliferate in response to TCR/costimulator engagement, as measured by tritiated thymidine incorporation (Fig. 2*A*) and CFSE dilution assays (Fig. *2B–G*). CD8 (Fig. 2*B–E* and not shown), but not CD4 (Fig. 2*F*, 2*G*), T cells underwent fewer cell divisions in response to TCR/CD28 engagement at both 48 (Fig. 2*B–E*) and 72 h (Fig. 2*A* and data not shown) poststimulation. Indeed, cav-$1^{-/-}$ CD8 T cells stimulated with plate-bound Abs to CD3/CD28 underwent approximately half as many divisions within the first 48 h (Fig. 2*D*). Fewer cav-$1^{-/-}$ CD8 T cells were found to reside in populations undergoing one, two, and three divisions, indicating defective coupling of TCR/ CD28 engagement to proliferation rather than a selective inability to undergo multiple divisions (Fig. 2*C*). Consistent with this interpretation, caveolin-1–deficient CD8 T cells retained the ability to divide in response to PMA/ionomycin stimulation (Fig. 2*E*), known to bypass TCR/CD28 engagement through direct activation calcium flux and protein kinase C (PKC) activation. Conversely, CD4 T cells isolated from cav-$1^{-/-}$ mice proliferated as well as wild-type CD4 cells in response to a range of TCR/CD28-specific Ab concentrations and at both 48 and 72 h (Fig. 2*F*, 2*G* and data not shown). These findings identify a unique requirement for caveolin-1 in coupling TCR/CD28 engagement to T cell proliferation in CD8, but not CD4, T cells.

To determine whether caveolin-1 plays a role in CD8 T cell effector function, we analyzed the effects of caveolin-1 gene knockout on IFN-γ production. After 72 h of TCR/CD28 stimulation, we found a lower percentage of IFN-γ–producing CD8 T cells in the later divisions of cultured CFSE-labeled cav-$1^{-/-}$ CD8 T cells (Fig. 2*H*). Published reports indicate that IFN-γ effector function is greater in cells that have undergone several divisions (36), thus fewer IFN-γ–producing cells is an expected secondary effect of impaired T cell division. However, even among those cav-$1^{-/-}$ CD8 T cells successfully undergoing four or more divisions, fewer cells were capable of producing IFN-γ, reflecting a defect in TCR-induced IFN-γ production extending beyond defective CD8 T cell proliferation.

To further investigate CD8 T cell effector function, we performed Ab-dependent cellular cytotoxicity (ADCC) assays using wild-type and cav-$1^{-/-}$ CD8 CTLs. Purified CD8 T cells from wild-type and cav-$1^{-/-}$ mice were stimulated with Abs to TCR/ CD28 for 3 d, and then tested for ADCC. Although cav-$1^{-/-}$ CD8 cells demonstrated some cytolytic activity, this activity was significantly reduced compared with wild-type cells (Fig. 2*I*). Because CTL activity was assessed on a per-CD8 T cell basis, our findings indicate that even those

cav-1$^{-/-}$ CD8 T cells that do divide and survive are defective in coupling TCR/CD28 engagement to the development or triggering of CD8 T effector function.

Caveolin-1 promotes Ag-induced membrane raft synaptic polarity and actin polymerization in CD8$^+$ T cells

Caveolin-1 can stabilize membrane raft microdomains by organizing membrane rafts and maintaining raft cell-surface expression (37). These activities have been implicated in caveolin-1 control of cell polarity in other cell types (38, 39). To determine whether caveolin-1 expression influences polarized membrane raft accumulation at the immune synapse, we compared the redistribution of the raft-associated glycolipid GM1 to synaptic contacts formed between caveolin-1–sufficient and –deficient OT-1 TCR-transgenic CD8 T cells and specific Ag/APC. As predicted, GM1-containing membrane rafts were polarized toward OT-1 T cell–APC synapses within 30 min of stimulation (Fig. 3*A*, *top panel*). In contrast, synaptic raft polarization was impaired in caveolin-1–de-ficient OT-1 CD8 T cells (Fig. 3*A*, *bottom panel*).

The redistribution of membrane rafts to the immune synapse is known to require TCR mediated actin polymerization (2). Therefore, we assessed a role for caveolin-1 in Ag/APC-induced actin polymerization by quantitating increases in polymerized F-actin. As shown in Fig. 3*B*, F-actin levels are similar between unstimulated wild-type and caveolin-1–deficient OT-1$^+$CD8 T cells. Ag/APC stimulation led to an increase in F-actin levels in wild-type OT-1$^+$CD8 T cells when compared with unstimulated cells (Fig. 3*B*). In contrast, caveolin-1–deficient OT-1$^+$CD8 T cells did not polymerize actin as efficiently as wild-type cells (Fig. 3*B*). This experiment is representative of three similar experiments. However, in one experiment, actin levels peaked earlier than in the other two, thus, to obtain statistics demonstrating significance, peak values from three experiments were averaged (Fig. 3*C*). Together, these findings demonstrate a role for caveolin-1 in coordinating Ag-induced actin polymerization and promoting Ag-induced membrane raft polarization at the immune synapse.

Caveolin-1 selectively regulates gene expression induced by TCR engagement in CD8, but not CD4, T cells

NFAT and NF-κB are key transcription factors that control the expression of genes activated by TCR/costimulator engagement. Thus, to determine whether caveolin-1 plays a role coupling TCR engagement to downstream NFAT or NF-κB activity, we measured mRNA expression of NFAT and NF-κB–regulated target genes (Nfatc1 and IκBα, respectively) in CD8 and CD4 T cells stimulated with either Abs to CD3/CD28 or PMA/ionomycin. Caveolin-1 deficiency in CD8 T cells resulted in selective disruption of TCR/CD28 upregulation of NFATc1, but not IκBα mRNA expression, compared with wild-type CD8 T cells (Fig. 4*A*). Accordingly, caveolin-1–deficient CD8 T cells were defective at upregulating NFAT-dependent TNF-α, IFN-γ, and IL-2 mRNA expression in response to TCR engagement (Fig. 4*A*). These data elucidate a role for caveolin-1 in directing TCR signal specificity. Consistent with our findings that caveolin-1 deficiency impacted TCR-induced proliferation in CD8, but not CD4, T cells, cav-1$^{-/-}$ CD8 T cells, but not cav-1$^{-/-}$ CD4 T cells, were selectively impaired in TCR signaling to NFAT-dependent TNF-α cytokine gene expression (Fig. 4*B*). Responses to PMA/ionomycin remained intact.

Re-expression of caveolin-1 in primary caveolin-1–deficient T cells using a retroviral expression construct led to enhancement of TCR-mediated upregulation of NFATc1 mRNA (Fig. 4*C*). These findings corroborate a role for caveolin-1 in coupling TCR engagement to upregulation of gene expression and indicate that defects observed in CD8 T cells result

from the direct loss of caveolin-1 and are not strictly due to secondary or compensatory effects of caveolin-1 gene knockout.

Caveolin-1 is required for optimal CD8 T cell Ag-induced expansion and function in vivo

To determine whether caveolin-1 regulates CD8 T cell expansion and viral clearance in vivo, wild-type and cav-$1^{-/-}$ mice were infected with the Armstrong strain of LCMV, which is known to enter cells through a mechanism independent of caveolin-1 (40). $GP^{33–41}/D^b$ tetramers were used to track the expansion of virus-specific CD8 T cells on days 5, 7, 9, and 12 postinfection (Fig. 5*A–D*). Seven days postinfection, cav-$1^{-/-}$ mice had significantly reduced numbers of CD8 T cells in their spleens compared with wild-type mice (Fig. 5*C*). Accordingly, spleens from cav-$1^{-/-}$ mice had lower percentages and absolute numbers of D^b $GP_{33–41}$ tetramer-positive CD8 T cells relative to spleens from wild-type mice on day 7 (Fig. 5*A*, 5*B*, 5*D*). Further, specific expansion of D^b $GP_{33–41}$-reactive CD8 T cells was delayed in cav-$1^{-/-}$ spleens, peaking at days 9–12 rather than at days 7–9 as seen in wild-type spleens (Fig. 5*B*). These data indicate that caveolin-1 expression facilitates timely Ag-specific CD8 T cell expansion in response to infection in vivo.

Next, we examined the ability of virus-specific CD8 T cells to produce IFN-γ in response to Ag. Splenocytes from wild-type and cav-$1^{-/-}$ mice were restimulated ex vivo with $GP_{33–41}$ and $NP_{396–404}$ peptide and levels of intracellular IFN-γ detected by FACS (Fig. 6). LCMV-infected cav-$1^{-/-}$ mice showed a lower percentage and total number of responding CD8 T cells producing IFN-γ in response to $GP_{33–41}$ (Fig. 6*A*, *left panels*, and data not shown) and $NP_{396–404}$ peptide (Fig. 6*A*, *right panels*, 6*B*) compared with wild-type LCMV-infected mice.

Viral plaque assays showed increased viral titers in the spleens of cav-$1^{-/-}$ mice 5 d postinfection (Fig. 6*C*) at a time when wild- type animals had already cleared the virus. Although both wild-type and cav-$1^{-/-}$ mice ultimately cleared virus by day 7 (data not shown), these data highlight the relevance of caveolin-1 expression for timely and efficient viral clearance in vivo. Taken together, these results show that caveolin-1 is important for the generation of efficient CD8 CTL immune responses and viral clearance in vivo.

Because caveolin-1 is expressed by several other cells controlling immunity, such as B cells and APCs (19, 41), we next determined if the defects in T cell responsiveness observed in caveolin-1–deficient mice were due to the specific loss of caveolin-1 in CD8 T cells. To this end, purified wild-type or cav-$1^{-/-}$ OT-1^+CD8 T cells were transferred into wild-type C57BL/6 recipient mice, and chimeric mice were immunized with *actA*-deficient LM-OVA 1 d later. $OVA_{257–264}/K^b$ tetramers were used to track the expansion of Ag-specific OT-1^+CD8 T cells at day 6 postinfection. Fewer tetramer-positive CD8 T cells had expanded in the spleens of mice that received cav-$1^{-/-}$ CD8 donor T cells in response to antigenic stimulation relative to mice that received wild-type CD8 donor T cells (Fig. 7*A–C*). Further, fewer cav-$1^{-/-}$ CD8 T cells responded to Ag stimulation by producing IFN-γ, whereas no differences in cytokine production were seen in response to PMA/ionomycin stimulation (Fig. 7*D*, 7*E*). These findings demonstrate that caveolin-1 regulation of CD8 T cell immunity can be directly attributed to expression of caveolin-1 in CD8 T cells.

Discussion

In this study, we demonstrate that primary T cells express caveolin-1. Caveolin-1 protein was detected in freshly isolated thymocytes and CD4 and CD8 subpopulations from spleen and lymph node. Detection of caveolin-1 protein in wild-type but not knockout T lineage cells, using three independent well-characterized Abs, rules out potential artifacts due to Ab cross-reactivity with other proteins. PCR amplification of cDNA made from CD4 and CD8

T cell subpopulations using caveolin-1–specific primers further validate our results. These findings are in contrast to the initial and widely cited reports that T lineage cells and lymphocytes, in general, do not express caveolin-1 (28–32). These reports were largely based on assessment of caveolin-1 expression in transformed cells, which may have lost caveolin-1 during the course of transformation or culture. Alternatively, the relatively low expression levels in T lineage cells may account for the reported lack of detection using less sensitive techniques. More recent evidence has shown that caveolin-1 is expressed in other immune cells including murine macrophages and mast cells (41), human and bovine dendritic cells (41), murine B cells (42), human, rat and murine neutrophils (41), activated T cell leukemia lines (43, 44), and bovine T cells (41). Additional expression profiling in thymocyte and effector T subsets will be necessary to determine if all T lineage cells express caveolin-1 or whether varying levels of caveolin-1 throughout development might function as a mechanism of setting subset-specific TCR thresholds or membrane trafficking.

To investigate a potential role for caveolin-1 in T cell maturation and function, we assessed T cell subset profiles and activity in caveolin-1–deficient C57BL/6 and OT-1 TCR-transgenic C57BL/6 mice. Analysis of thymocyte and peripheral T cell developmental and activation markers including CD3, CD4, CD8 CD25, CD69, CD62L, and CD5 demonstrated normal numbers and relative percentages of thymic and peripheral T cell subsets defined by their expression, indicating that caveolin-1 expression is not essential for T cell development. No overt autoimmunity or immune deficiency was observed in these mice in the absence of antigenic challenge, consistent with findings that thymocyte development or mature T lymphocyte homeostasis is not grossly altered.

In assessing TCR/CD28 responsiveness in mature peripheral CD4 and CD8 T cell subsets lacking caveolin-1, we found that CD8, but not CD4, T cells were uniquely affected by caveolin-1 deficiency, despite its expression in both subsets. Freshly isolated caveolin-1–deficient CD8 T cells demonstrated defective TCR-induced actin polymerization, synaptic polarity, and NFAT-dependent NFATc1 and effector cytokine transcription and proliferation. Accordingly, re-expression of caveolin-1 in deficient primary CD8 T cells enhanced downstream NFATc1 transcription, ruling out the possibility that the effects of caveolin-1 deficiency in CD8 T cells are strictly secondary to compensatory mechanisms during the course of development. Further, cav-$1^{-/-}$ CD8 T cells remain competent to respond to PMA/ionomycin by proliferating and inducing NFATc1 and effector cytokine transcription. These findings demonstrate that caveolin-1 CD8 T cells are defective at coupling TCR/CD28 engagement to downstream signal transduction and effector activation and pinpoint the lesion as lying upstream or independent of Ca^{++} flux and PKC activation pathways. Alternatively, TCR coupling to NF-κB–responsive IκBα gene transcription remains intact, elucidating a role for caveolin-1 in selectively guiding TCR/CD28 signal specificity toward activation of a subset of available downstream pathways. Re-expression of caveolin-1 in caveolin-1–deficient CD8 T cells only partially reconstituted TCR-induced NFATc1 transcription, leaving open the possibility that caveolin-1 deficiency might also impair CTL development. Each of the outputs affected by caveolin-1 deficiency were significantly diminished, but not ablated, in the caveolin-1 knockout CD8 T cells, consistent with a role for caveolin-1 in setting TCR signaling thresholds and guiding signal specificity rather than as an essential TCR transducer scaffold.

In other cell systems, caveolin-1 promotes the stability of cell-surface membrane rafts and directs membrane dynamics and polarity (reviewed in Refs. 24, 26). Caveolin-1 can directly impact membrane dynamics by binding and shuttling cholesterol to the plasma membrane and through interaction with sphingolipids including GM1 (21, 24) or indirectly by coordinating signal transducers that regulate the actin cytoskeleton and/or membrane traffic (23, 24). The actin-mediated polarized redistribution of membrane rafts to the T cell–APC

contact is proposed to guide synaptic composition and assembly and potentiate TCR signal transduction by concentrating and organizing transducers within membrane specializations (1, 2). We found that caveolin-1 ablation diminishes the trafficking of membrane raft microdomains to the T cell– APC contact. Caveolin-1 ablation also impairs Ag induced actin polymerization required for synaptic raft redistribution. Therefore, we propose that caveolin-1 regulation of TCR-induced actin and membrane dynamics at the synapse might specialize the synapse for recruitment and activation of transducer assemblies required for coupling TCR engagement to NFAT-dependent and potentially other downstream signal transduction pathways.

Caveolin-1 has been characterized as a protein scaffold that directly binds and controls the activity of Csk, Fyn, PP1/PP2a, dynamin-2, and filamin-A, each of which have been implicated in mediating CD28/TCR-induced signals, membrane dynamic, and functions impacted in caveolin-1–deficient T cells (14, 17, 18, 20, 27). Caveolin-1 also binds Ras, PKC-θ, heterotrimeric G proteins, and other transducers with capacities to influence TCR signal transduction (7, 8, 10, 13). Although caveolin-1 has been linked to Csk activity in other cell types (12), we were unable to distinguish differences in Lck 505 phosphorylation status in resting or stimulated caveolin-1 wild-type versus deficient CD8 T cells in preliminary experiments (T. Tomassian and M.C. Miceli, unpublished observations). Similar to dynamin 2 ablation (45), caveolin-1 deficiency impacted Ag-induced actin reorganization, but not TCR internalization prior to or after engagement (T. Tomassian and M.C. Miceli, unpublished observations). It is noteworthy that filamin-A also physically associates with CD28 and integrins and is required for CD28-mediated recruitment of membrane rafts to the immune synapse (46). Bruton's tyrosine kinase–caveolin-1 complexes have been identified in B cells (42). The sites responsible for the interactions of Bruton's tyrosine kinase and Fyn with caveolin-1 are conserved in ITK and Lck family members required for efficient T cell activation, actin polymerization, and NFAT signaling (47). Thus, ITK and Lck represent additional candidate caveolin-1 effectors.

Although similarities between T cells lacking caveolin-1 and T cells lacking these potential T cell-binding partners are striking, in no case does the ablation of any single transducer perfectly recapitulate the effects observed in caveolin-1 knockout mice (45– 48). Scaffolding proteins have emerged as key central organizers of multicomponent signaling complexes in numerous systems, creating focal points for control of signal transduction cascades. Therefore, it is likely that caveolin-1 acts through multiple binding partners, positioning them for select participation in a subset of available signal transduction cascades. Future studies assessing which potential caveolin-1 interactions are intact in CD8 and CD4 T cells and the affects of caveolin-1 on their contributions to TCR/ CD28-mediated signal transduction should help elucidate the molecular basis of caveolin-1 activity in CD8 T cells and may provide an explanation for its select contributions to TCR/CD28 signaling dynamics in CD8, but not CD4, T cells.

By infecting caveolin-1–deficient mice with LCMV and tracking Ag-specific CD8 T cells, we demonstrated that caveolin-1 is required for efficient CD8 T cell Ag-specific expansion and effector function in vivo. Though caveolin-1–deficient CD8 T cells expanded with a delayed kinetic, responding cells were shown to be less efficient at producing IFN-γ. These defects translated into defective viral clearance, highlighting the biological relevance of caveolin-1 in regulating CD8 T cell responses in vivo. Similar results were seen in OT-1 T cell expansion and effector function after adoptive transfer into wild-type hosts and stimulation with LM-OVA, demonstrating that caveolin-1 expression in CD8 T cells is directly responsible for observed CD8 defects. Together, these findings identify caveolin-1 as a novel positive regulator of CD8-mediated responses to viral and bacterial pathogens in vivo. Previous reports have identified a role for caveolin-1 in regulating B cell and

macrophage responses (42, 49, 50), though contributions to regulating T cell responsiveness have not been previously noted. Accordingly, findings that caveolin-1–deficient mice are more susceptible to *Salmonella* and parasitic infections have been attributed to defective macrophage activity and inflammatory responses (49, 50). In light of our findings demonstrating a role for cavolin-1 in regulating T cell immunity, defective T cell responsiveness might also contribute to these previously reported defects.

In conclusion, we have identified caveolin-1 as a specifier of T cell polarity, synaptic composition, TCR signal transduction, and functional output that is selectively employed in different T cell subsets to customize T cell responses. These findings support the emerging view that protein and membrane scaffolds serve as points of control for setting signaling thresholds and modulating TCR output (2, 4). Thus, future studies elucidating mechanisms of pathway activation coordinated by scaffolds may elucidate targets for selective manipulation of particular TCR signals and T effector functions.

Supplementary Material

Refer to Web version on PubMed Central for supplementary material.

Acknowledgments

We thank members of the Miceli laboratory for critical reading of the manuscript.

T.T. is a recipient of Microbial Pathogenesis Training Grant 2-T32-AI-07323. L.A.H. is a recipient of an Arthritis Foundation Postdoctoral Fellowship. S.D.L. was supported by the Microbial Pathogenesis Training Grant T32-AI07323-15, Clinical and Fundamental Training Grant AI07126-30, and a Warsaw Fellowship. This work was supported by R01-AI067253-10 (to M.C.M.) and AI085043 (to D.G.B.) from the National Institutes of Health.

Abbreviations used in this article

ADCC	Ab-dependent cellular cytotoxicity
LCMV	lymphocytic choriomeningitis virus
LM-OVA	*Listeria monocytogenes-OVA*
PKC	protein kinase C

References

1. Friedl P, den Boer AT, Gunzer M. Tuning immune responses: diversity and adaptation of the immunological synapse. Nat. Rev. Immunol. 2005; 5:532–545. [PubMed: 15999094]
2. Miceli MC, Moran M, Chung CD, Patel VP, Low T, Zinnanti W. Co-stimulation and counter-stimulation: lipid raft clustering controls TCR signaling and functional outcomes. Semin. Immunol. 2001; 13:115–128. [PubMed: 11308295]
3. Fooksman DR, Vardhana S, Vasiliver-Shamis G, Liese J, Blair DA, Waite J, Sacristán C, Victora GD, Zanin-Zhorov A, Dustin ML. Functional anatomy of T cell activation and synapse formation. Annu. Rev. Immunol. 2010; 28:79–105. [PubMed: 19968559]
4. Rebeaud F, Hailfinger S, Thome M. Dlgh1 and Carma1 MAGUK proteins contribute to signal specificity downstream of TCR activation. Trends Immunol. 2007; 28:196–200. [PubMed: 17395537]
5. Moran M, Miceli MC. Engagement of GPI-linked CD48 contributes to TCR signals and cytoskeletal reorganization: a role for lipid rafts in T cell activation. Immunity. 1998; 9:787–796. [PubMed: 9881969]
6. Cannon JL, Burkhardt JK. The regulation of actin remodeling during T-cell-APC conjugate formation. Immunol. Rev. 2002; 186:90–99. [PubMed: 12234365]

7. Oka N, Yamamoto M, Schwencke C, Kawabe J, Ebina T, Ohno S, Couet J, Lisanti MP, Ishikawa Y. Caveolin interaction with protein kinase C. Isoenzyme-dependent regulation of kinase activity by the caveolin scaffolding domain peptide. J. Biol. Chem. 1997; 272:33416–33421. [PubMed: 9407137]
8. Song KS, Li Shengwen T, Okamoto LA, Quilliam Sargiacomo M, Lisanti MP. Co-purification and direct interaction of Ras with caveolin, an integral membrane protein of caveolae microdomains. Detergent-free purification of caveolae microdomains. J. Biol. Chem. 1996; 271:9690–9697. [PubMed: 8621645]
9. Li S, Seitz R, Lisanti MP. Phosphorylation of caveolin by src tyrosine kinases. The alpha-isoform of caveolin is selectively phosphorylated by v-Src in vivo. J. Biol. Chem. 1996; 271:3863–3868. [PubMed: 8632005]
10. Li S, Okamoto T, Chun M, Sargiacomo M, Casanova JE, Hansen SH, Nishimoto I, Lisanti MP. Evidence for a regulated interaction between heterotrimeric G proteins and caveolin. J. Biol. Chem. 1995; 270:15693–15701. [PubMed: 7797570]
11. Abulrob A, Giuseppin S, Andrade MF, McDermid A, Moreno M, Stanimirovic D. Interactions of EGFR and caveolin-1 in human glio-blastoma cells: evidence that tyrosine phosphorylation regulates EGFR association with caveolae. Oncogene. 2004; 23:6967–6979. [PubMed: 15273741]
12. Cao H, Sanguinetti AR, Mastick CC. Oxidative stress activates both Src-kinases and their negative regulator Csk and induces phosphorylation of two targeting proteins for Csk: caveolin-1 and paxillin. Exp. Cell Res. 2004; 294:159–171. [PubMed: 14980511]
13. Engelman JA, Chu C, Lin A, Jo H, Ikezu T, Okamoto T, Kohtz DS, Lisanti MP. Caveolin-mediated regulation of signaling along the p42/44 MAP kinase cascade in vivo. A role for the caveolin-scaffolding domain. FEBS Lett. 1998; 428:205–211. [PubMed: 9654135]
14. Yao Q, Chen J, Cao H, Orth JD, McCaffery JM, Stan RV, McNiven MA. Caveolin-1 interacts directly with dynamin-2. J. Mol. Biol. 2005; 348:491–501. [PubMed: 15811383]
15. Schubert AL, Schubert W, Spray DC, Lisanti MP. Connexin family members target to lipid raft domains and interact with caveolin-1. Biochemistry. 2002; 41:5754–5764. [PubMed: 11980479]
16. Uittenbogaard A, Smart EJ. Palmitoylation of caveolin-1 is required for cholesterol binding, chaperone complex formation, and rapid transport of cholesterol to caveolae. J. Biol. Chem. 2000; 275:25595–25599. [PubMed: 10833523]
17. Stahlhut M, van Deurs B. Identification of filamin as a novel ligand for caveolin-1: evidence for the organization of caveolin-1-associated membrane domains by the actin cytoskeleton. Mol. Biol. Cell. 2000; 11:325–337. [PubMed: 10637311]
18. Li L, Ren CH, Tahir SA, Ren C, Thompson TC. Caveolin-1 maintains activated Akt in prostate cancer cells through scaffolding domain binding site interactions with and inhibition of serine/threonine protein phos-phatases PP1 and PP2A. Mol. Cell. Biol. 2003; 23:9389–9404. [PubMed: 14645548]
19. Vargas L, Nore BF, Berglof A, Heinonen JE, Mattsson PT, Smith CI, Mohamed AJ. Functional interaction of caveolin-1 with Bruton's tyrosine kinase and Bmx. J. Biol. Chem. 2002; 277:9351–9357. [PubMed: 11751885]
20. Sanguinetti AR, Cao H, Corley Mastick C. Fyn is required for oxidative- and hyperosmotic-stress-induced tyrosine phosphorylation of caveolin-1. Biochem. J. 2003; 376:159–168. [PubMed: 12921535]
21. Smart EJ, Ying Y, Donzell WC, Anderson RG. A role for caveolin in transport of cholesterol from endoplasmic reticulum to plasma membrane. J. Biol. Chem. 1996; 271:29427–29435. [PubMed: 8910609]
22. Liu P, Li WP, Machleidt T, Anderson RG. Identification of caveolin-1 in lipoprotein particles secreted by exocrine cells. Nat. Cell Biol. 1999; 1:369–375. [PubMed: 10559965]
23. Lajoie P, Goetz JG, Dennis JW, Nabi IR. Lattices, rafts, and scaffolds: domain regulation of receptor signaling at the plasma membrane. J. Cell Biol. 2009; 185:381–385. [PubMed: 19398762]
24. Sonnino S, Prinetti A. Sphingolipids and membrane environments for caveolin. FEBS Lett. 2009; 583:597–606. [PubMed: 19167383]
25. Simons K, Toomre D. Lipid rafts and signal transduction. Nat. Rev. Mol. Cell Biol. 2000; 1:31–39. [PubMed: 11413487]

26. Liu P, Rudick M, Anderson RG. Multiple functions of caveolin-1. J. Biol. Chem. 2002; 277:41295–41298. [PubMed: 12189159]
27. Cao H, Courchesne WE, Mastick CC. A phosphotyrosine-dependent protein interaction screen reveals a role for phosphorylation of caveolin-1 on tyrosine 14: recruitment of C-terminal Src kinase. J. Biol. Chem. 2002; 277:8771–8774. [PubMed: 11805080]
28. Fra AM, Williamson E, Simons K, Parton RG. Detergent-insoluble glycolipid microdomains in lymphocytes in the absence of caveolae. J. Biol. Chem. 1994; 269:30745–30748. [PubMed: 7982998]
29. Xavier R, Brennan T, Li Q, McCormack C, Seed B. Membrane compartmentation is required for efficient T cell activation. Immunity. 1998; 8:723–732. [PubMed: 9655486]
30. Harder T, Simons K. Caveolae, DIGs, and the dynamics of sphingolipid-cholesterol microdomains. Curr. Opin. Cell Biol. 1997; 9:534–542. [PubMed: 9261060]
31. Nabi IR, Le PU. Caveolae/raft-dependent endocytosis. J. Cell Biol. 2003; 161:673–677. [PubMed: 12771123]
32. Alonso MA, Millán J. The role of lipid rafts in signalling and membrane trafficking in T lymphocytes. J. Cell Sci. 2001; 114:3957–3965. [PubMed: 11739628]
33. Round JL, Tomassian T, Zhang M, Patel V, Schoenberger SP, Miceli MC. Dlgh1 coordinates actin polymerization, synaptic T cell receptor and lipid raft aggregation, and effector function in T cells. J. Exp. Med. 2005; 201:419–430. [PubMed: 15699074]
34. Elsaesser H, Sauer K, Brooks DG. IL-21 is required to control chronic viral infection. Science. 2009; 324:1569–1572. [PubMed: 19423777]
35. van der Most RG, Sette A, Oseroff C, Alexander J, Murali-Krishna K, Lau LL, Southwood S, Sidney J, Chesnut RW, Matloubian M, Ahmed R. Analysis of cytotoxic T cell responses to dominant and sub-dominant epitopes during acute and chronic lymphocytic choriomeningitis virus infection. J. Immunol. 1996; 157:5543–5554. [PubMed: 8955205]
36. Murali-Krishna K, Ahmed R. Cutting edge: naive T cells masquerading as memory cells. J. Immunol. 2000; 165:1733–1737. [PubMed: 10925249]
37. Smart EJ, Graf GA, McNiven MA, Sessa WC, Engelman JA, Scherer PE, Okamoto T, Lisanti MP. Caveolins, liquid-ordered domains, and signal transduction. Mol. Cell. Biol. 1999; 19:7289–7304. [PubMed: 10523618]
38. Grande-García A, Echarri A, de Rooij J, Alderson NB, Waterman-Storer CM, Valdivielso JM, del Pozo MA. Caveolin-1 regulates cell polarization and directional migration through Src kinase and Rho GTPases. J. Cell Biol. 2007; 177:683–694. [PubMed: 17517963]
39. Beardsley A, Fang K, Mertz H, Castranova V, Friend S, Liu J. Loss of caveolin-1 polarity impedes endothelial cell polarization and directional movement. J. Biol. Chem. 2005; 280:3541–3547. [PubMed: 15504729]
40. Rojek JM, Perez M, Kunz S. Cellular entry of lymphocytic choriomeningitis virus. J. Virol. 2008; 82:1505–1517. [PubMed: 18045945]
41. Hu G, Ye RD, Dinauer MC, Malik AB, Minshall RD. Neutrophil caveolin-1 expression contributes to mechanism of lung inflammation and injury. Am. J. Physiol. Lung Cell. Mol. Physiol. 2008; 294:L178–L186. [PubMed: 17993589]
42. Medina FA, Williams TM, Sotgia F, Tanowitz HB, Lisanti MP. A novel role for caveolin-1 in B lymphocyte function and the development of thymus-independent immune responses. Cell Cycle. 2006; 5:1865–1871. [PubMed: 16929183]
43. Hatanaka M, Maeda T, Ikemoto T, Mori H, Seya T, Shimizu A. Expression of caveolin-1 in human T cell leukemia cell lines. Biochem. Biophys. Res. Commun. 1998; 253:382–387. [PubMed: 9878546]
44. Tsuji Y, Hatanaka M, Maeda T, Seya T, Takenaka H, Shimizu A. Differential-expression and tyrosine-phosphorylation profiles of caveolin iso-forms in human T cell leukemia cell lines. Int. J. Mol. Med. 2005; 16:889–893. [PubMed: 16211260]
45. Gomez TS, Hamann MJ, McCarney S, Savoy DN, Lubking CM, Heldebrant MP, Labno CM, McKean DJ, McNiven MA, Burkhardt JK, Billadeau DD. Dynamin 2 regulates T cell activation by controlling actin polymerization at the immunological synapse. Nat. Immunol. 2005; 6:261–270. [PubMed: 15696170]

46. Tavano R, Contento RL, Baranda SJ, Soligo M, Tuosto L, Manes S, Viola A. CD28 interaction with filamin-A controls lipid raft accumulation at the T-cell immunological synapse. Nat. Cell Biol. 2006; 8:1270–1276. [PubMed: 17060905]

47. Lucas JA, Miller AT, Atherly LO, Berg LJ. The role of Tec family kinases in T cell development and function. Immunol. Rev. 2003; 191:119–138. [PubMed: 12614356]

48. Palacios EH, Weiss A. Function of the Src-family kinases, Lck and Fyn, in T-cell development and activation. Oncogene. 2004; 23:7990–8000. [PubMed: 15489916]

49. Bucci M, Gratton JP, Rudic RD, Acevedo L, Roviezzo F, Cirino G, Sessa WC. In vivo delivery of the caveolin-1 scaffolding domain inhibits nitric oxide synthesis and reduces inflammation. Nat. Med. 2000; 6:1362–1367. [PubMed: 11100121]

50. Medina FA, Cohen AW, de Almeida CJ, Nagajyothi F, Braunstein VL, Teixeira MM, Tanowitz HB, Lisanti MP. Immune dysfunction in caveolin-1 null mice following infection with *Trypanosoma cruzi* (Tulahuen strain). Microbes Infect. 2007; 9:325–333. [PubMed: 17317261]

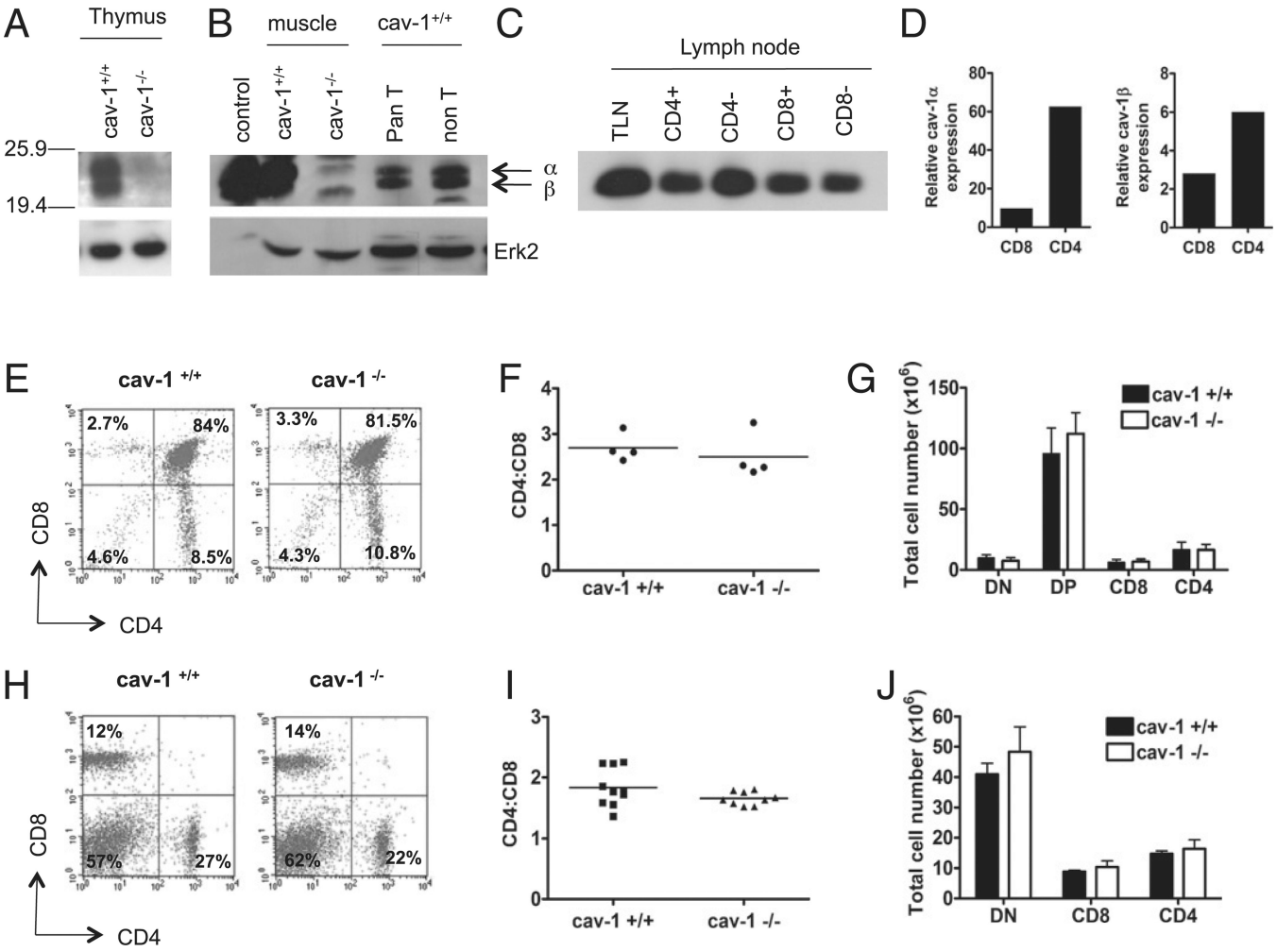

FIGURE 1.

Caveolin-1 is expressed in mouse T lineage cells, though caveolin-1–deficient mice develop typical $CD4^{-}CD8^{-}$, $CD4^{+}CD8^{+}$, $CD4^{+}$, and $CD8^{+}$ subpopulations in thymus and spleen. Total cell lysate from wild-type (cav-$1^{+/+}$) and caveolin-1–deficient (cav-$1^{-/-}$) thymocytes (*A*) or splenic (*B*) or lymph node (*C*) T or non-T cells were immunoblotted using Abs to the first 97 (1–97) aa of caveolin-1 (*A, B*) or against 20 aa in the N terminus of caveolin-1 (*C*), respectively. cav-$1^{+/+}$ and cav-$1^{-/-}$ endothelial muscle cell lysates serve as controls. Erk2 levels served as loading controls. *D*, RNA from purified CD4 and CD8 splenocytes from cav-$1^{+/+}$ and cav-$1^{-/-}$ mice was converted to cDNA and caveolin-1α and β mRNA levels determined using N-terminal–specific primers and quantitative PCR. Relative levels normalized to L32 are shown. *E–J*, CD4 and CD8 expression profiles on developing thymocyte subpopulations (*E*) and splenic T cells (*H*) from 6.2-wk-old cav-$1^{+/+}$ (*left panels*) and cav-$1^{-/-}$ (*right panels*) mice. The percentage of cells in each subset is denoted in its respective quadrant. The ratio of $CD4^{+}$ to $CD8^{+}$ thymocytes (*F*) or splenic T cells (*I*) from cav-$1^{+/+}$ (*left panels*) and cav-$1^{-/-}$ (*right panels*) mice are shown. *G*, The mean of the total cell numbers (± SD) for each thymic subpopulation was determined by multiplying the percentage of cells in each subset by the total number of thymocytes ($n = 4$ mice/genotype): cav-$1^{+/+}$ (black bar) and cav-$1^{-/-}$ (open bar). *H*, CD4 and CD8 flow profiles are representative of 10 independent mice. *J*, The mean of the total cell numbers (± SD) for each splenic T cell subpopulation.

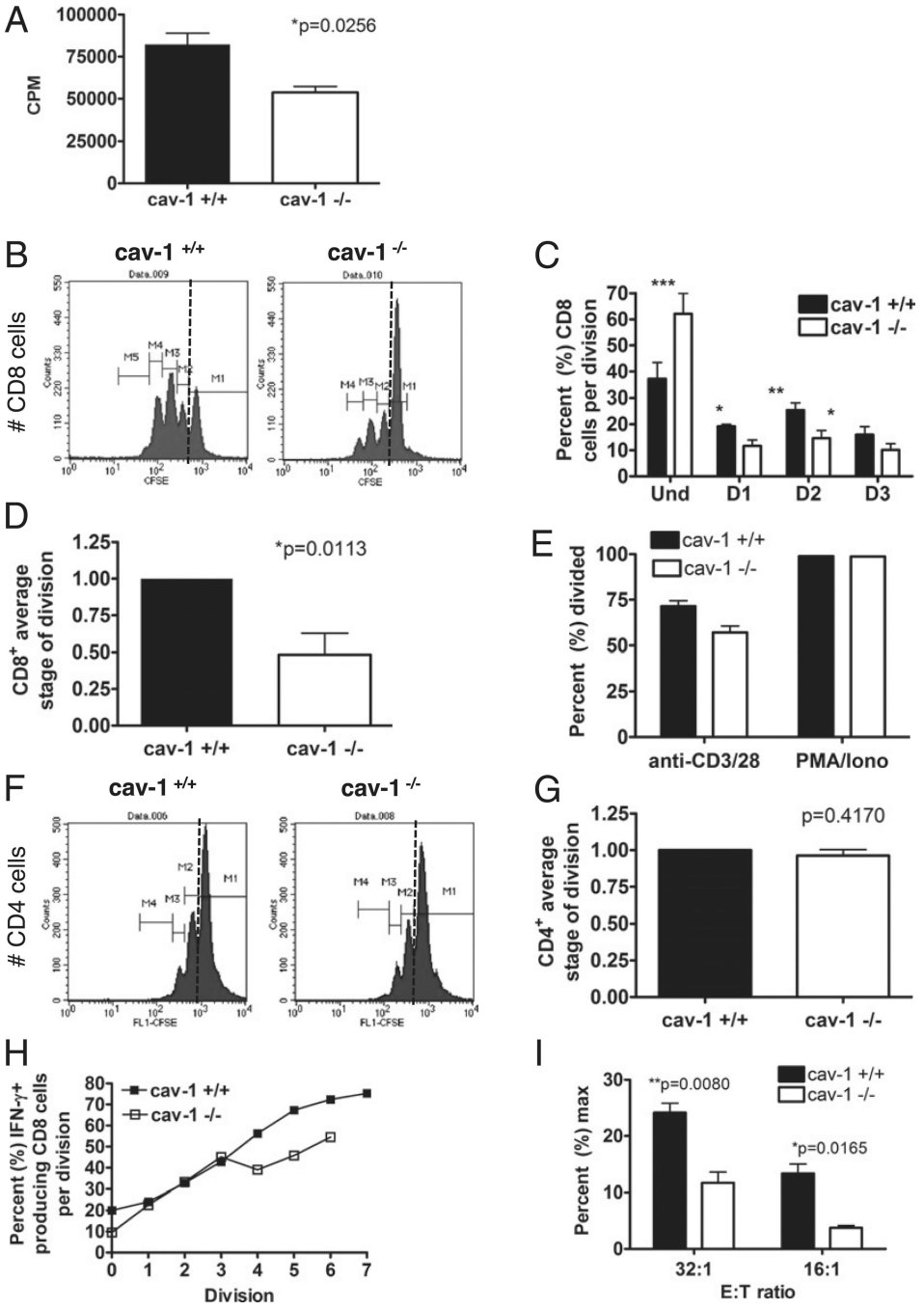

FIGURE 2.

Only caveolin-1–deficient $CD8^+$ T cells are defective at TCR/CD28-mediated proliferation and IFN-γ and CTL effector function. *A*, cav-$1^{+/+}$ (black bar) or cav-$1^{-/-}$ (white bar) CD8 cells stimulated for 72 h with CD3/CD28-specific Ab-conjugated beads and assessed for proliferation using thymidine incorporation assay. *B–I*, CFSE dilution profile of cav-$1^{+/+}$ (*left panels*) and cav-$1^{-/-}$ (*right panels*) CD8 (*B*) or CD4 (*F*) cells stimulated with plate-bound Ab to CD3/CD28 for 48 h. The dotted line separates undivided (*right panels*) from dividing (*left panels*) cells. The percent of cells in each division of CD8 (*B, C*) and CD4 (*F*) and average stage of division of CD8 (*D*) or CD4 (*G*) cav-$1^{+/+}$ (black bars) and cav-$1^{-/-}$

(open bars) cells was calculated. Data are representative of three and four independent experiments for CD8 and CD4 T cells, respectively. *E*, The percent of divided versus undivided cells in cultured cav-$1^{+/+}$ (black bars) and cav-$1^{-/-}$ (open bars) CD8 cells in response to CD3/CD28-specific Abs (*right panel*) or PMA/ionomycin (*left panel*) (PMA/ionomycin data: $n = 2$ cav-$1^{+/+}$ and $n = 3$ cav-$1^{-/-}$). *H*, The percent of IFN-γ–positive cells in each division of cav-$1^{+/+}$ (black squares) and cav-$1^{-/-}$ (open squares) CFSE-labeled CD8 cells stimulated with plate-bound Abs to CD3/CD28 for 72 h. *I*, ADCC activity of cav-$1^{+/+}$ (black bars) and cav-$1^{-/-}$ (open bars) CD8 cells directed against CD3-specific Ab-labeled P815 targets at various E:T ratios (E:T). Significance was determined using paired Student *t* test. *$p < 0.05$, **$p < 0.01$, ***$p < 0.001$.

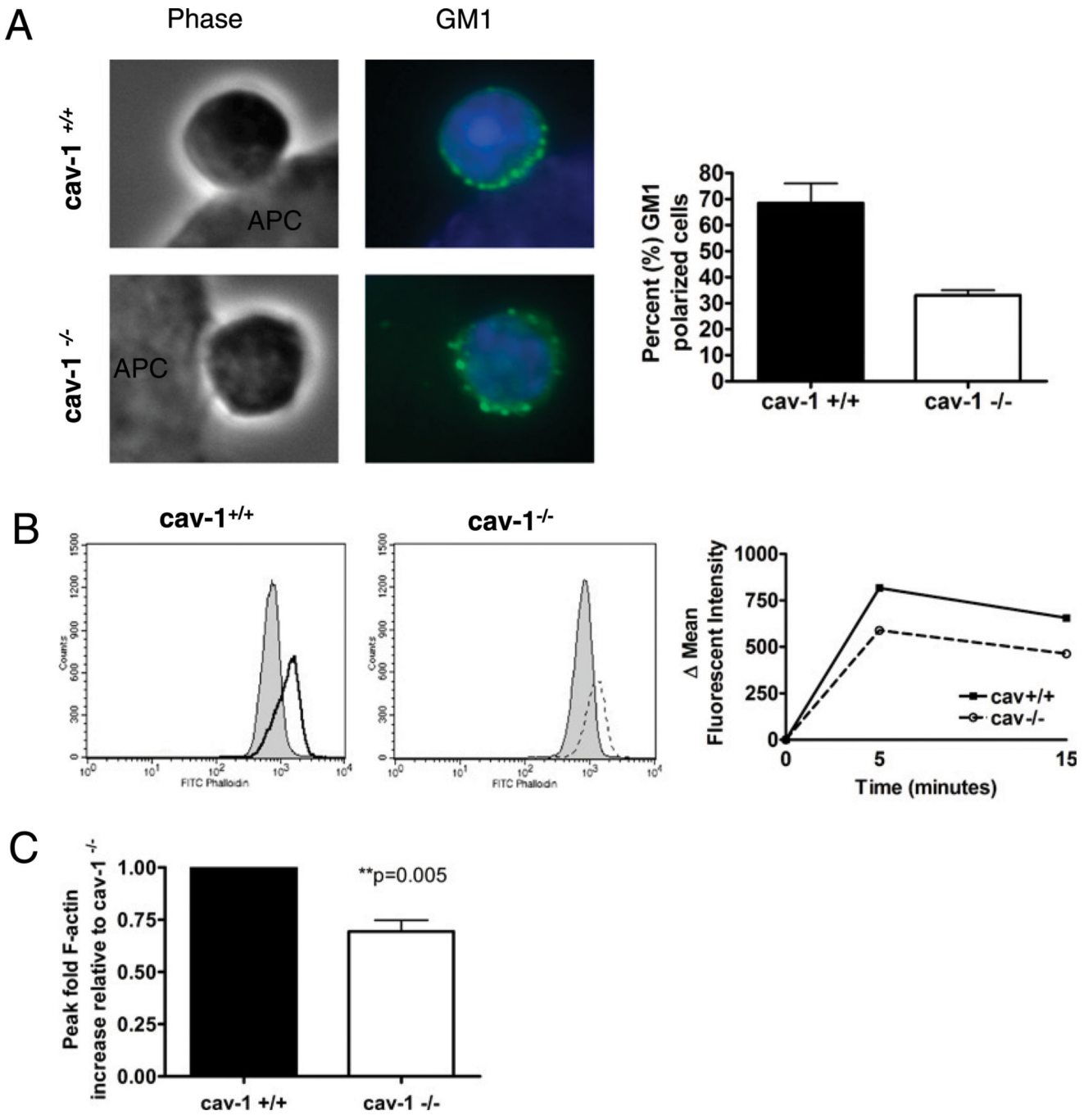

FIGURE 3.

Caveolin-1 promotes Ag-induced membrane raft synaptic polarization and actin polymerization in $CD8^+$ T cells. *A, Left panel*, Phase and fluorescent microscopy of raft-associated GM1 glycolipid localization in $CD8^+$ cells from OT-1 cav-$1^{+/+}$ and cav-$1^{-/-}$ mice stimulated with APCs expressing $OVA_{257–264}$ Ag for 30 min. *Right panel*, The percentage of cells with GM1 polarized at the synapse of OT-1 cav-$1^{+/+}$ (black bar) and cav-$1^{-/-}$ (open circle) $CD8^+$ cells. Cells were stained with FITC-conjugated Cholera Toxin β subunit and cells were imaged using a 63×/1.4 oil immersion objective lens. Mean and SD from two experiments was used to calculate percent GM1-polarized cells. Fifty T cell–APC

conjugates were counted per experiment, and cells were scored positive for synaptic clustering when >60% of the GM1 was polarized toward the T cell–APC junction. *B*, cav-$1^{+/+}$ (*left panel*) or cav-$1^{-/-}$ (*middle panel*) OT-1 T cells were incubated with OVA-expressing APCs for 5 or 15 min to stimulate actin polymerization. T cells were washed of APCs, fixed, and stained with FITC-conjugated phalloidin and analyzed by FACS. Change in actin was calculated (stimulated mean intensity minus unstimulated mean intensity, *B right panel*) and representative of three independent experiments. *C*, Mean and SD of fold change of F-actin was calculated from peak levels observed in three independent experiments.

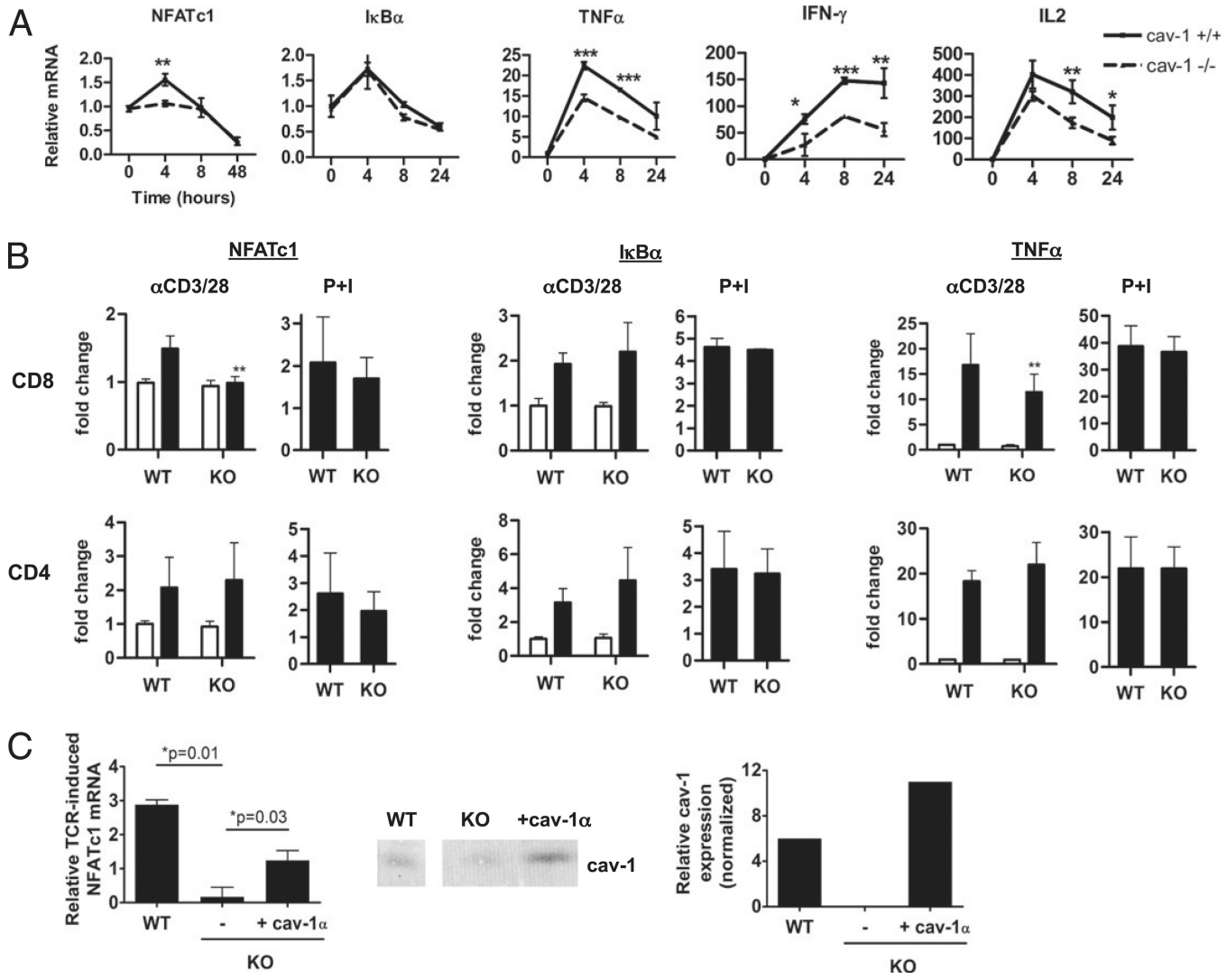

FIGURE 4.

Caveolin-1 selectively modulates TCR-induced transcriptional activation in $CD8^+$ T cells. *A*, Purified cav-$1^{+/+}$ (solid line) or cav-$1^{-/-}$ (dashed line) $CD8^+$ T cells were stimulated with Abs to CD3/CD28 and harvested at the various time points for gene expression analysis via quantitative RT-PCR; data are representative to two independent experiments. *B*, cav-$1^{+/+}$ or cav-$1^{-/-}$ $CD8^+$ (*top panels*) or $CD4^+$ (*bottom panels*) T cells were left unstimulated (open bars) or stimulated with either Ab to CD3/CD28 or PMA/ionomycin (black bars) for 4 h and analyzed as in *A*; shown is the average of two experiments (paired Student *t* tests were performed; *$p < 0.05$, **$p < 0.01$, ***$p < 0.001$). *C*, cav-$1^{+/+}$ or cav-$1^{-/-}$ OT-1 CD8 cells were expanded on APCs for 3 d and then left untransduced or retrovirally transduced with MIG–caveolin-1 retroviral vector. At 72 h posttransduction, cells were stimulated with plate-bound Ab to CD3/CD28 for 6 h. TCR-induced NFATc1 mRNA levels were quantitated and normalized to L32 mRNA levels (*left panel*). Cell lysates were immunoblotted with Abs to caveolin-1 (610406, mouse mAb; BD Pharmingen) (*middle panel*). Intensity of caveolin-1 bands was quantitated using Odyssey software and normalized to p38 levels. Numbers are shown relative to cav-$1^{-/-}$ (*right panel*).

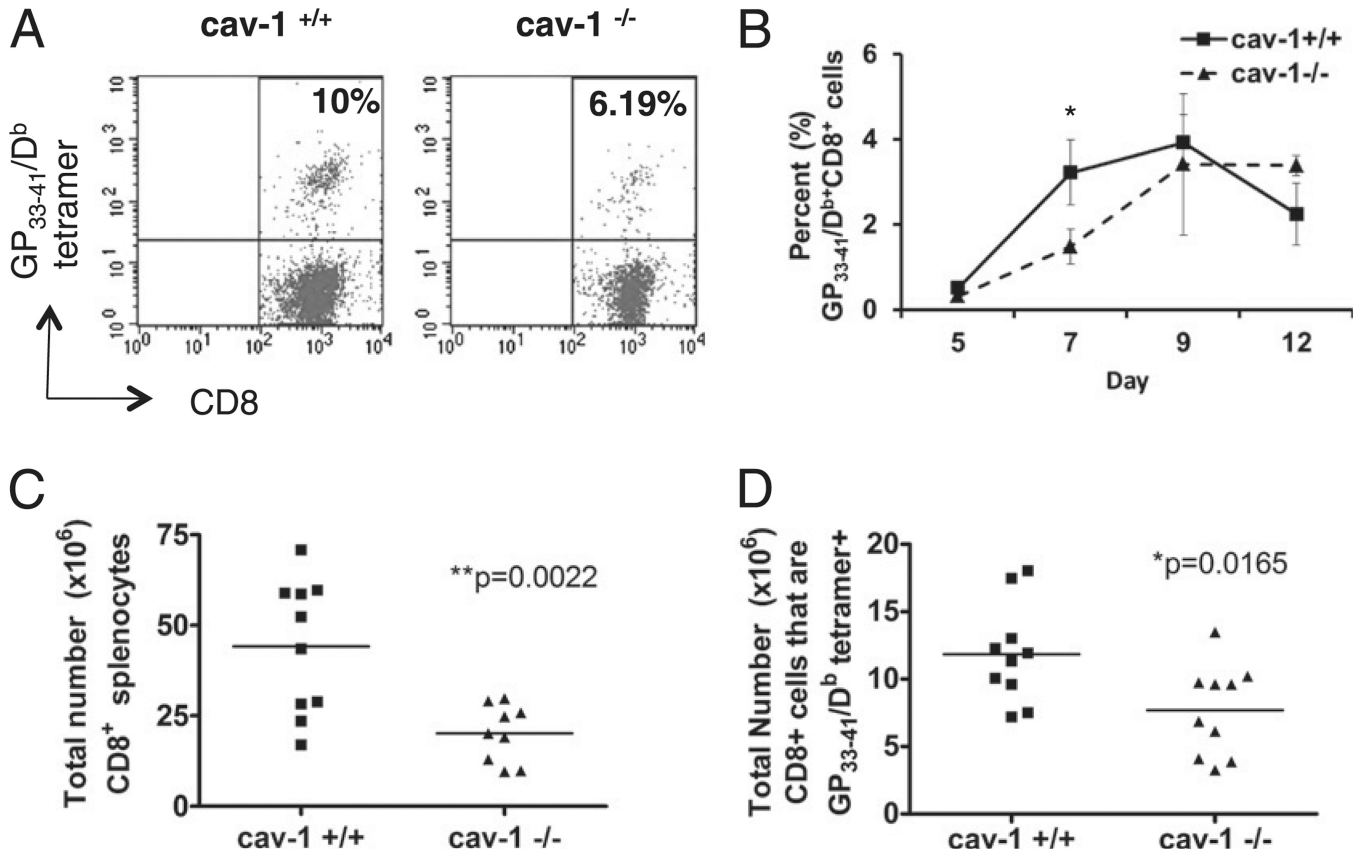

FIGURE 5.

Caveolin-1 knockout mice are deficient at Ag-specific $CD8^+$ T cell expansion in response to LCMV infection. *A*, Flow cytometry profiles (CD8 versus $GP_{33–41}/D^b$ tetramer) of $CD8^+$ gated splenocytes from day 7 post–LCMV-infected cav-$1^{+/+}$ (*left panel*) and cav-$1^{-/-}$ (*right panel*) mice. The percentage of tetramer-positive CD8 T cells is indicated in the upper right quadrant. *B*, The percentage of $CD8^+$ tetramer-positive cells from cav-$1^{+/+}$ (solid line, black squares) or Cav-$1^{-/-}$ (hatched line, black triangles) mice at day 5, 7, 9, and 12 postinfection. Bars represent SD of T cell responses from a single experiment with three independent wild-type and cav-$1^{-/-}$ mice. Similar results were seen in two independent experiments. *C*, The total number of $CD8^+$ cells in the spleens of cav-$1^{+/+}$ (black squares) and cav-$1^{-/-}$ (black triangles) mice. *D*, The total number of CD8 T cells that are tetramer positive from cav-$1^{+/+}$ (black squares) or cav-$1^{-/-}$ (black triangles) mice at day 7 postinfection. Total cell numbers were determined by multiplying the total number of splenocytes by the percentage of $CD8^+$ T cells (*C*) or $CD8^+$ T cells that were $GP_{33–41}/D^b$-positive (*D*). T cell responses from 3 independent experiments and 14 independent cav-$1^{+/+}$ and cav-$1^{-/-}$ mice 7 d postinfection with LCMV are shown in *C* and *D*. Significance was determined using paired Student *t* test. $*p < 0.05$, $**p < 0.01$.

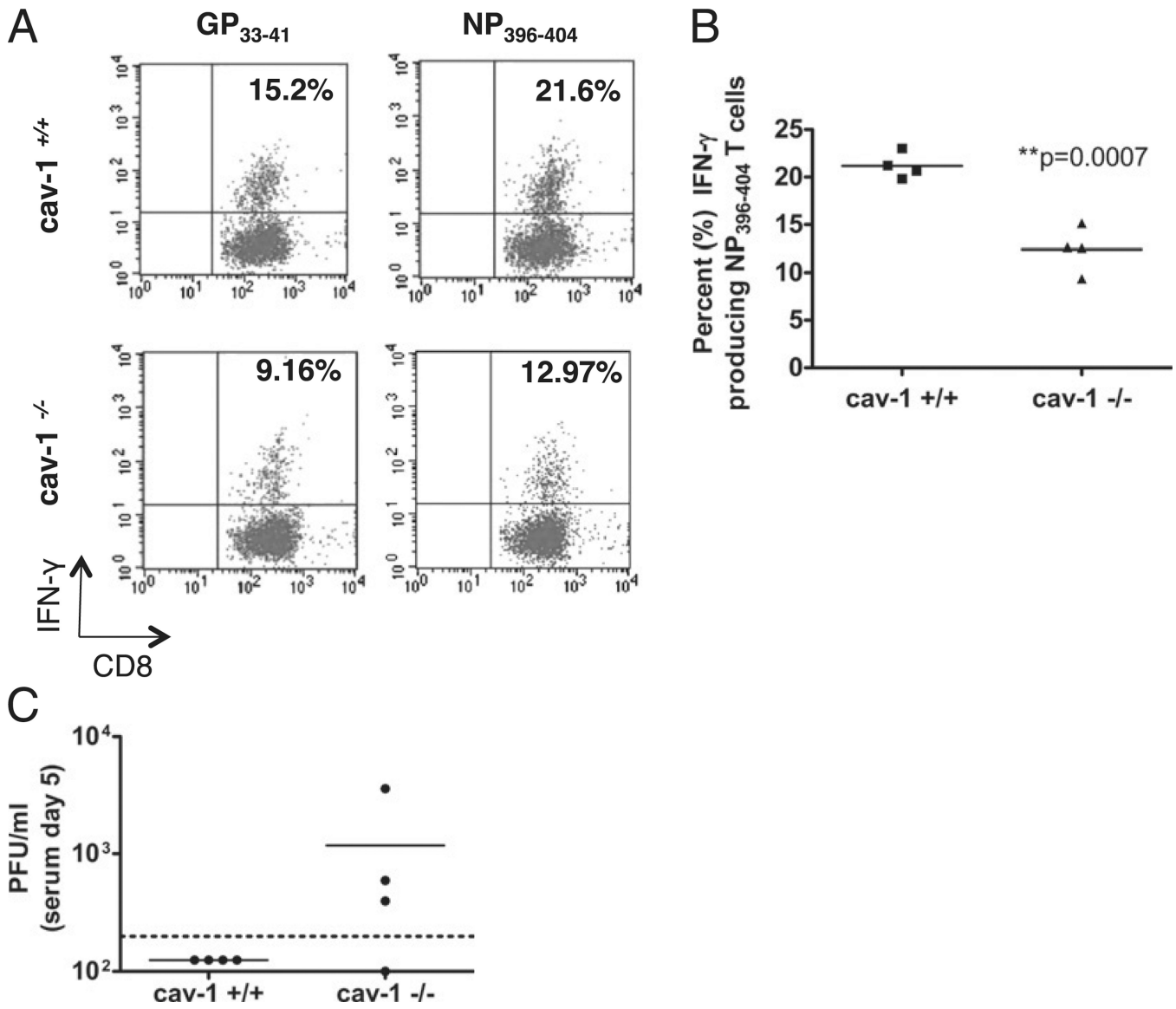

FIGURE 6.

Caveolin-1 expression is required for generation of optimal virus-specific $CD8^+$ T cell function and viral clearance. Cav-$1^{+/+}$ and cav-$1^{-/-}$ mice were injected with 2×10^5 PFU LCMV Armstrong strain i.p. *A*, Flow profiles (CD8 versus IFN-γ) of day 7 postinfection splenocytes stimulated with $GP_{33–41}$ (*left panel*) and $NP_{396–404}$ peptide (*right panel*) ex vivo for 5 h. The percentage of CD8 T cells that are IFN-γ positive is indicated in the upper right quadrant. *B*, The percentage of cav-$1^{+/+}$ (black squares) and cav-$1^{-/-}$ (black triangles) CD8 cells making IFN-γ after restimulation with $NP_{396–404}$ peptide. *C*, Viral titer from serum of day 5 postinfection cav-$1^{+/+}$ (black squares) and cav-$1^{-/-}$ (black triangles) mice obtained from eight mice in two independent experiments. Viral titers were calculated using a standard plaque assay.

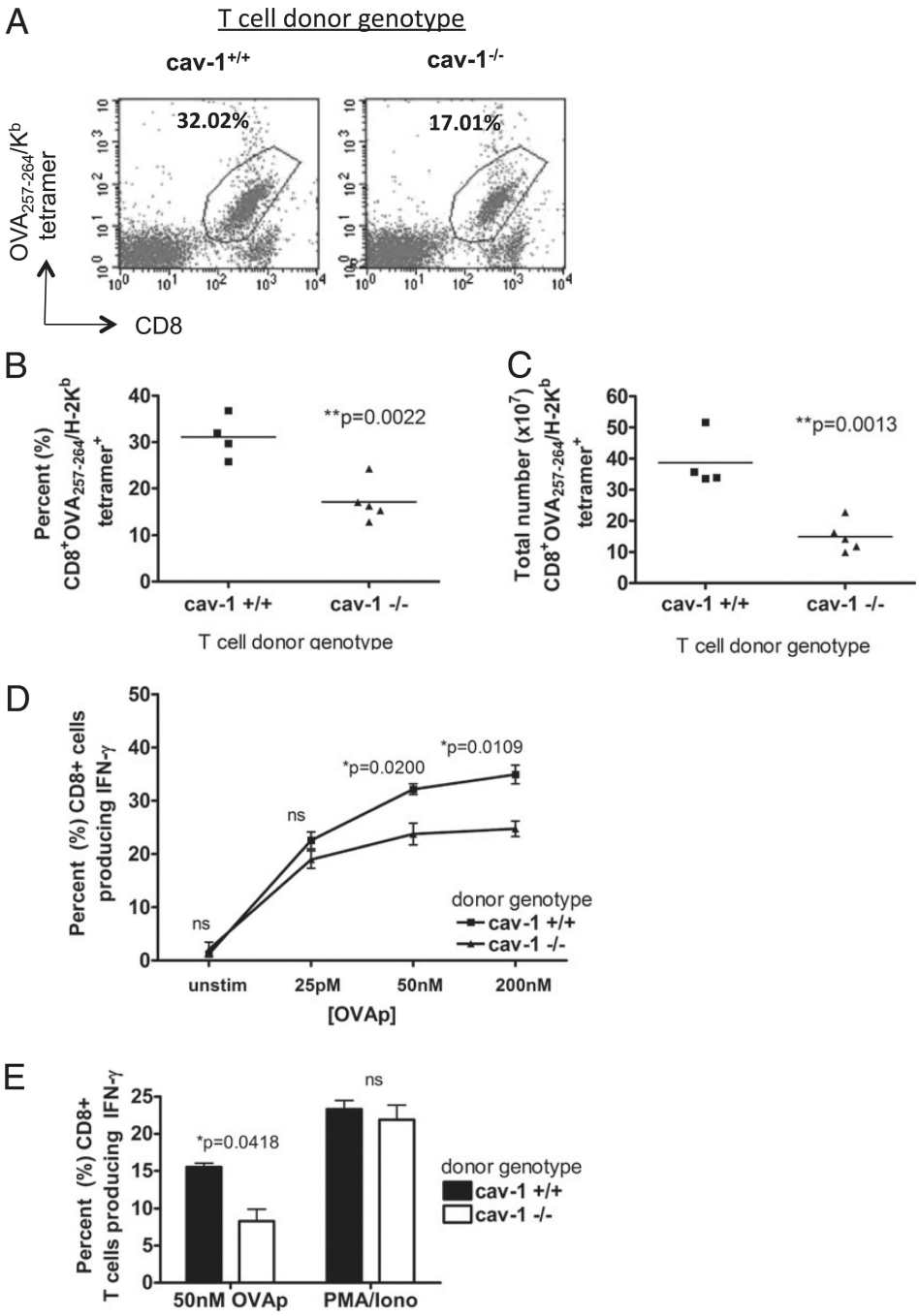

FIGURE 7.

Caveolin-1 expression by Ag-specific $CD8^+$ T cells is required for optimal $CD8^+$ T cell expansion and effector function in vivo. Purified cav-$1^{+/+}$ or cav-$1^{-/-}$ OT-1 $CD8^+$ T cells were adoptively transferred into wild-type C57BL/6 mice that were immunized with *actA*-deficient LM-OVA 1 d later. *A*, Flow profiles (CD8 versus $OVA_{257–264}/K^b$ tetramer) of splenocytes from mice that received cav-$1^{+/+}$ (*left panel*) and cav-$1^{-/-}$ (*right panel*) OT-1 $CD8^+$ donor cells 6 d after immunizing with *actA*-deficient LM-OVA. The circled region indicates percentage of tetramer-positive $CD8^+$ cells. Percent (*B*) and total number (*C*) of tetramer-positive CD8 T cells from mice that received cav-$1^{+/+}$ (black squares) or cav-$1^{-/-}$

(black triangles) OT-1^{+}CD8 donor T cells. Values were determined by multiplying the total number of splenocytes by the percent of $OVA_{257–264}/K^{b}$ tetramer-positive CD8 cells. *D* and *E*, The percentage of cav-$1^{+/+}$ (black squares) and cav-$1^{-/-}$ (black triangles) OT-1^{+}CD8 donor T cells making IFN-γ after restimulation with $OVA_{257–264}$ peptide or PMA/ionomycin.